

Article

Determining the Rheological Parameters of Polymers Using Artificial Neural Networks

Anton Chepurnenko 

Strength of Materials Department, Faculty of Civil and Industrial Engineering, Don State Technical University, 344003 Rostov-on-Don, Russia; anton_chepurnenk@mail.ru; Tel.: +7-863-201-9136

Abstract: Artificial neural networks have great prospects in solving the problems of predicting the properties of polymers. The purpose of this work was to study the possibility of using artificial neural networks to determine the rheological parameters of polymers from stress relaxation curves. The nonlinear Maxwell–Gurevich equation was used as the deformation law. The problem was solved in the MATLAB environment. The substantiation for the choice of the neural network input and output parameters was made. An algorithm for obtaining the data for neural network training was also proposed. Neural networks were trained on theoretical stress relaxation curves constructed with the Euler method. The value of the mean square error (MSE) was used as a criterion for the performance of the training. The constructed model of the artificial neural network was tested on the experimental relaxation curves of recycled polyvinyl chloride. The quality of the experimental curve approximation was quite good and was comparable with the standard methods for processing stress relaxation curves. Unlike the standard methods, when using artificial neural networks, no preliminary data smoothing was required. It is possible to use the proposed technique for processing not only relaxation curves, but also creep curves as well as processing creep tests not only in central tension, but also in bending, torsion and shear.

Keywords: creep; relaxation; artificial neural networks; rheological parameters; polyvinyl chloride



Citation: Chepurnenko, A. Determining the Rheological Parameters of Polymers Using Artificial Neural Networks. *Polymers* **2022**, *14*, 3977. <https://doi.org/10.3390/polym14193977>

Academic Editors: Chao-Tsai Huang, Sheng-Jye Hwang and Hsinshu Peng

Received: 31 August 2022

Accepted: 21 September 2022

Published: 23 September 2022

Publisher's Note: MDPI stays neutral with regard to jurisdictional claims in published maps and institutional affiliations.



Copyright: © 2022 by the author. Licensee MDPI, Basel, Switzerland. This article is an open access article distributed under the terms and conditions of the Creative Commons Attribution (CC BY) license (<https://creativecommons.org/licenses/by/4.0/>).

1. Introduction

Pronounced creep is characteristic for many polymers and composites based on them in addition to the elastic properties. For use in products for various purposes, it is important to be able to determine the rheological properties of polymer materials. In most existing techniques, the rheological parameters of polymers are determined from tests for creep under central tension [1–4]. The phenomenon of stress relaxation in polymers is interrelated with the phenomenon of creep and can be described by the same laws [5]; therefore, the rheological parameters of polymeric materials can also be determined from stress relaxation experiments [6–9].

One of the simplest rheological models, which is applied not only to polymers, but also to other materials such as concrete and wood, is the Maxwell–Thompson linear model. The creep strain ε^* growth rate in this model under a uniaxial stress state is determined by the following expression [10]:

$$\frac{\partial \varepsilon^*}{\partial t} = \frac{1}{nE} \left[\left(1 - \frac{H}{E} \right) \sigma - H\varepsilon^* \right] \quad (1)$$

where σ is the stress, t is the time, E is the instant modulus of elasticity, H is the long modulus of elasticity and n is the relaxation time.

The product $n \cdot E$ is also called the relaxation viscosity η^* . In Equation (1), the viscosity is constant and does not depend on stress, which does not fully reflect the existing experimental data.

For many polymers, including polypropylene, polyvinyl chloride, high and low density polyethylene and polyurethane, a better agreement with the experimental data is provided by the nonlinear Maxwell–Gurevich equation, in which viscosity depends on stress [11–15]:

$$\frac{\partial \varepsilon^*}{\partial t} = \frac{f^*}{\eta^*} \quad (2)$$

$$f^* = \sigma - E_\infty \varepsilon^* \quad (3)$$

$$\frac{1}{\eta^*} = \frac{1}{\eta_0^*} \exp\left(\frac{|f^*|}{m^*}\right) \quad (4)$$

Here, f^* is the stress function, E_∞ is the high elasticity modulus, η_0^* is the initial relaxation viscosity and m^* is the velocity modulus.

A more complex structure of the creep equation complicates the processing of the experimental data. The existing traditional methods for processing creep and relaxation curves based on the Maxwell–Gurevich equation [16,17] use numerical differentiation and require a sufficiently high quality of experimental curves.

Machine learning methods have great prospects in solving inverse problems, including the determination of the mechanical properties of materials. An artificial neural network (ANN) is one of the artificial intelligence methods that provides solutions for classification and regression problems. It is known as one of the best methods for data mining tasks. ANNs learn to predict output data using a set of attributes. The purpose of an ANN is to find solutions to problems in the same way that the human brain does [18].

Works [19–21] are examples of determining the properties of pavement materials with the help of an ANN. Papers [22,23] propose a method for determining the chemical, physical and mechanical properties of polymers based on their molecular structure using machine learning methods. In [24], artificial neural networks are used to predict the glass transition temperature of polymers based on their structure. Paper [25] proposes an optimized artificial intelligence model to predict the kerf quality characteristics in the laser cutting of basalt fibers reinforced with polymer composites. In [26], a new hybrid artificial intelligence approach is proposed to model the ultrasonic welding of a polymeric material blend. In [27], an ANN is used as one of the methods for predicting the properties of bistable morphing composites.

The possibilities of artificial neural networks are far from being exhausted.

The aim of this work was to study the possibility of using artificial neural networks to determine the rheological parameters of polymers based on the nonlinear Maxwell–Gurevich equation. The stress relaxation experiment was taken as a basis, but the approach could also be applied to the processing of the results of experiments on creep under central tension and other simple types of deformation such as bending, torsion and shear. The novelty of the proposed approach lay primarily in the choice of input parameters for the neural network as well as in the method of obtaining the data on which the neural network was then trained.

2. Materials and Methods

Figure 1 shows a typical relaxation curve constructed with the Maxwell–Gurevich equation. Let us single out the characteristic points on this curve that were used as the input variables in the neural network: σ_0 is the stress at the initial moment of time; σ_∞ is the stress at the end of the relaxation process (at $t \rightarrow \infty$); and t_n is the time during which the stress drop $\Delta\sigma$ is:

$$\Delta\sigma = \sigma(t_n) - \sigma_0 = (\sigma_0 - \sigma_\infty) \left(1 - \frac{1}{e}\right) \quad (5)$$

It is shown in [28] that, in the case of using the Maxwell–Gurevich equation, the relationship between stresses and strains at $t \rightarrow \infty$ has the form:

$$\sigma_{\infty} = H\varepsilon \quad (7)$$

where $H = E \cdot E_{\infty} / (E + E_{\infty})$ is the long modulus of elasticity.

Thus, if the values of ε and σ_{∞} are known, then it is not difficult to find the long modulus H . From the known values of E and H , one can then find E_{∞} using the formula:

$$E_{\infty} = \frac{E \cdot H}{E - H} \quad (8)$$

Determining the values m^* and η_0^* is associated with further difficulties and an artificial neural network may be used for this. The input parameters of the network were the values ε , σ_0 , σ_{∞} , t_n and t_{95} . At the output, the network should produce the parameters m^* and η^* .

Network training was performed on the theoretical relaxation curves. For this, the possible ranges of change were selected in the modulus of elasticity $E \in [E_1; E_2]$, high elasticity modulus $E_{\infty} \in [E_{\infty 1}; E_{\infty 2}]$, velocity modulus $m^* \in [m_1^*; m_2^*]$, initial relaxation viscosity $\eta_0^* \in [\eta_{01}^*; \eta_{02}^*]$ and deformation $\varepsilon \in [\varepsilon_1; \varepsilon_2]$. For each parameter in the specified ranges, the m values were generated and evenly spaced on the numerical axis. For E , E_{∞} , m^* and η_0^* , we took 20 values; for ε , we took 3 standard values (1, 2 and 3%). Thus, the total number of options was $20^4 \times 3 = 480,000$. For each option, a theoretical stress relaxation curve was constructed with the Euler method. The algorithm used for constructing the theoretical curve was as follows:

1. The long modulus of elasticity was calculated $H = E \cdot E_{\infty} / (E + E_{\infty})$;
2. The stress σ_{∞} was calculated by Formula (7);
3. The maximum creep strain at $t \rightarrow \infty$ was determined by the formula:

$$\varepsilon_{max}^* = \frac{\sigma_{\infty}}{E_{\infty}} \quad (9)$$

4. The number of steps for the creep deformation n_{ε} was set (we took it as equal to 200) and the step size was calculated:

$$\Delta\varepsilon^* = \frac{\varepsilon_{max}^*}{n_{\varepsilon}} \quad (10)$$

5. The creep strain growth rate at $t = 0$ was determined:

$$\frac{\partial\varepsilon^*}{\partial t} = \frac{\sigma_0}{\eta_0^*} \cdot \exp\left(\frac{\sigma_0}{m^*}\right) \quad (11)$$

6. The time step was calculated:

$$\Delta t = \frac{\Delta\varepsilon^*}{\frac{\partial\varepsilon^*}{\partial t}} \quad (12)$$

7. The creep strain at time $t + \Delta t$ was then determined by the formula:

$$\varepsilon_{t+\Delta t}^* = \varepsilon_t^* + \frac{\partial\varepsilon^*}{\partial t} \Delta t \quad (13)$$

8. The stresses at time $t + \Delta t$ were determined by the formula:

$$\sigma = E(\varepsilon - \varepsilon^*) \quad (14)$$

9. The strain growth rate was then calculated from the stresses using Formula (2).

Points (7)–(9) were then repeated until the creep strain reached the value ε_{max}^* . For each constructed curve, it was possible to determine the values t_n and t_{95} . Two data arrays were then formed—*input* $5 \times 480,000$ in size and *target* $2 \times 480,000$ in size—on which the neural network was trained. The *input* array columns contained the values ε , σ_0 , σ_∞ , t_n and t_{95} for each calculated option. The *target* array columns contained the corresponding m^* and η_0^* values.

The implementation of the neural network was made in the MATLAB environment. A feed-forward backpropagation network with one layer of hidden neurons was chosen as the network type. The number of hidden neurons varied from 10 to 14. The network architecture is shown in Figure 3. The input layer had 5 neurons, according to the number of input parameters. Each of the neurons of the input layer was connected to the neurons of the hidden layer by synapses with weights w_i . The neurons in the hidden layer transformed the signals coming from the input layer using an activation function. We used TANSIG (the hyperbolic tangent sigmoid transfer function) as an activation function in MATLAB. From the neurons of the hidden layer, the converted signal went to the neurons of the output layer. The neural network training process was the adjustment of the weights of the synapses [18].

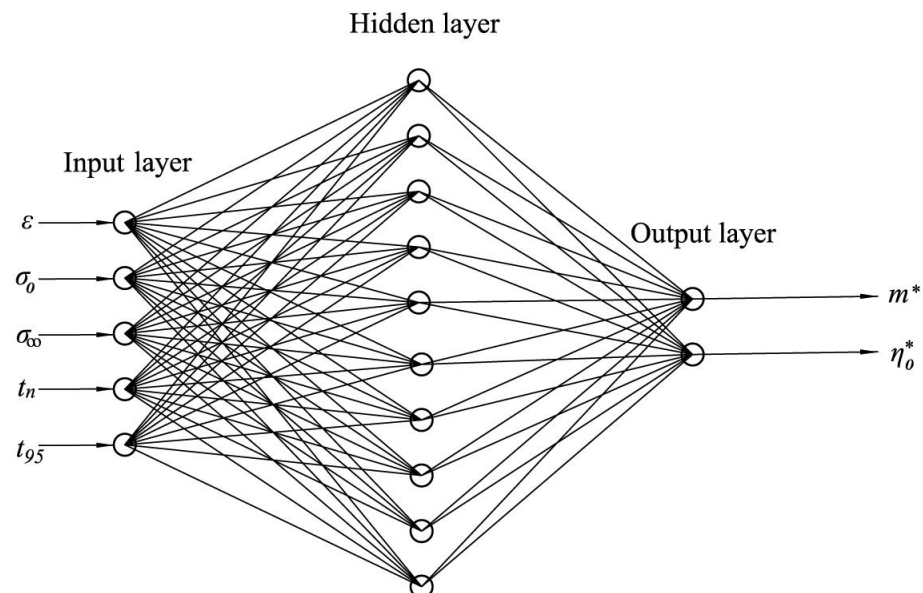


Figure 3. Neural network architecture.

The Levenberg–Marquardt method was used to adjust the weights of the network. There were four main functions for the evaluation of the training performance in MATLAB:

1. MSE (mean square error):

$$MSE = \frac{1}{n_s} \sum_{i=1}^{n_s} (d_i - y_i)^2 \quad (15)$$

where y_i is the current value of the variable at the output of the network, d_i is the target value and n_s is the total number of output values for the considered sample.

2. MSEREG (mean squared error with regularization performance function). It measured the network performance as the weight sum of two factors: the mean squared error and the mean squared weight and bias values.
3. SSE (sum squared error):

$$SSE = \sum_{i=1}^{n_s} (d_i - y_i)^2 \quad (16)$$

4. MAE (mean absolute error):

$$MAE = \frac{1}{n_s} \sum_{i=1}^{n_s} |d_i - y_i| \quad (17)$$

We chose the value of the MSE as the criterion for the training performance.

3. Results

An approximation of the technique for relaxation curve processing was carried out on the relaxation curves of the recycled polyvinyl chloride presented in [29]. In this work, the tests were carried out at a level of deformation of $\varepsilon = 3\%$. The temperature in the experiment T changed from 20 to 70 °C with a step of 10 °C. The dependence of stresses on the time at different temperatures is shown in Table 1.

When training the neural network, the range of change in the elastic modulus E was taken from 400 to 4000 MPa; in the high elasticity modulus E_∞ , the range was from $0.05 \cdot E$ to $4 \cdot E$, the velocity modulus m^* varied from 1 to 15 MPa and the initial relaxation viscosity varied from 10^6 to 10^8 MPa·s. The generated data were randomly divided into three parts: training; validation; and testing in proportions of 70%, 15% and 15%.

The optimal number of neurons in the hidden layer turned out to be 12. The neural net training performance graph is shown in Figure 4. When using the network with 12 neurons in the hidden layer, the best validation performance was 47.71 after 1000 iterations. Due to the large amount of data generated for training, the mean square errors for the samples "Train", "Validation" and "Test" were almost the same. A further increase in the number of neurons led to the overtraining of the model. The regression charts of the model with 12 neurons are shown in Figure 5. For several input parameter values, there was a rather large deviation between the output predicted and the target values, which could be explained by the large sample size and wide range of input parameters. The correlation coefficients R between the output and the target values averaged 0.977. A value of the correlation coefficient close to 1 was one of the indicators of the possibility of using the model in the forecasting process.

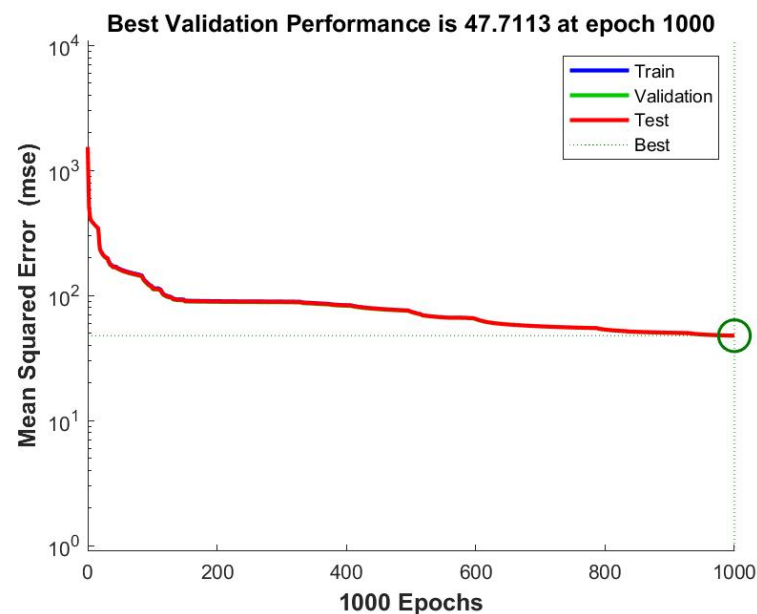


Figure 4. Neural net training performance graph.

Table 1. Time dependence of stresses at different temperatures.

Time, Minutes	0	3	6	15	30	45	60	90	120	180	
<i>T</i> , °C											
	20	44.4	40.8	39.8	38.8	38.0	37.7	37.3	36.9	36.4	35.6
	30	43.4	36.7	35.7	34.3	33.0	32.2	31.9	30.8	30.3	29.2
σ , MPa	40	39.3	32.9	31.4	29.0	27.0	25.9	24.9	23.8	22.7	21.3
	50	36.4	20.5	18.8	16.5	14.7	13.9	13.0	12.5	11.9	11.1
	60	33.4	15.4	13.4	10.6	8.61	7.63	6.95	6.02	5.42	5.05
	70	23.4	5.06	4.05	2.84	2.48	2.16	2.00	1.85	1.58	1.31

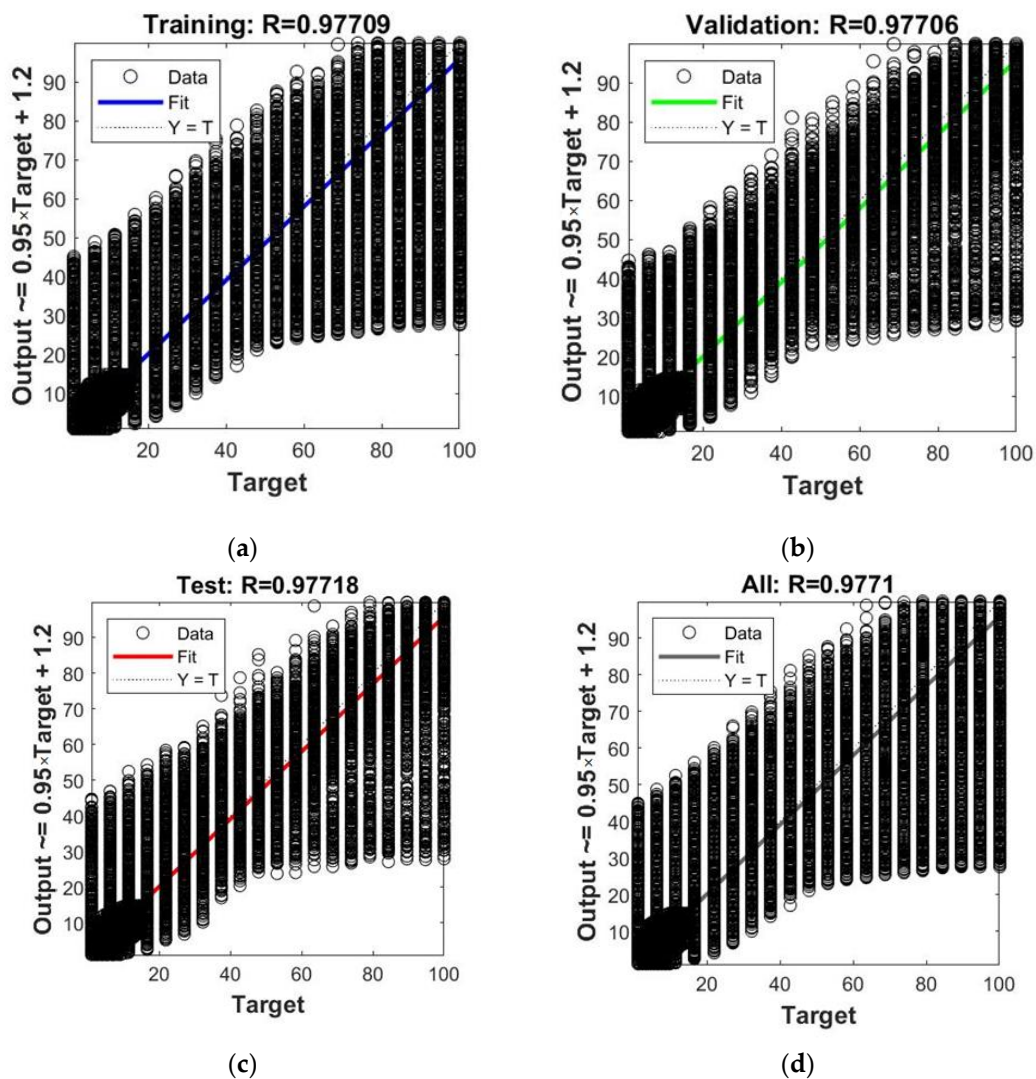


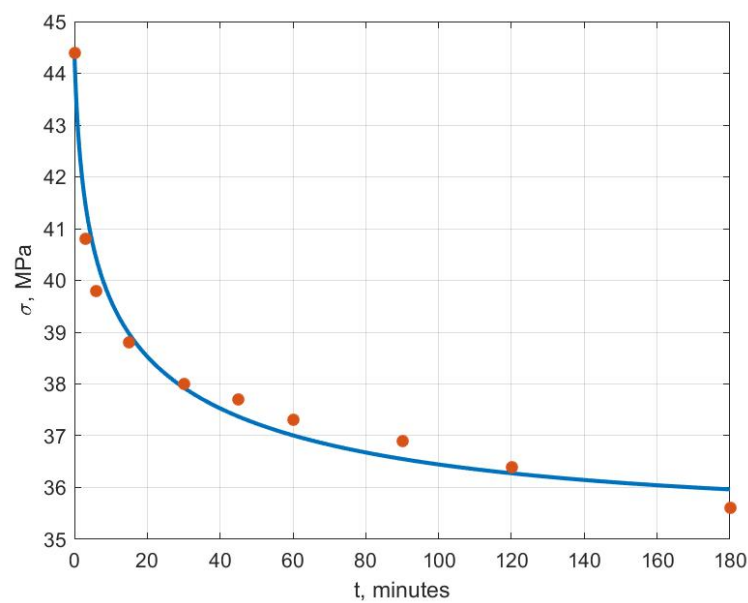
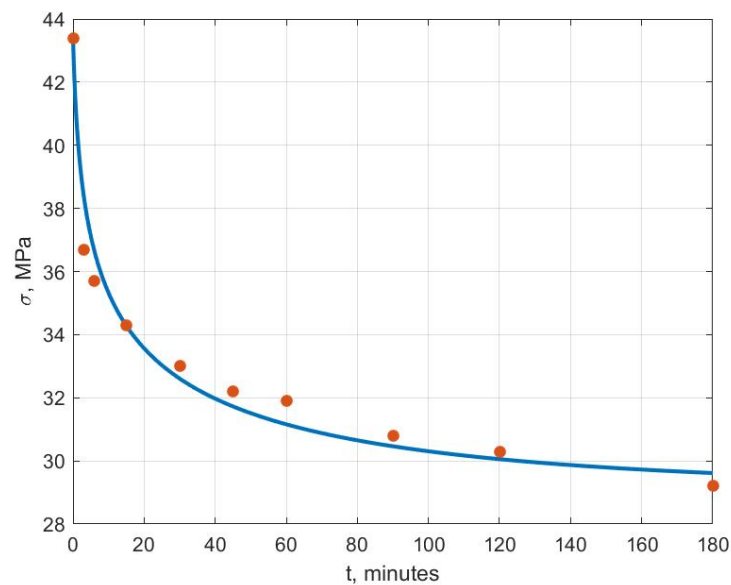
Figure 5. Regression charts for model with 12 hidden neurons: (a) Training sample; (b) Validation sample; (c) Test sample; (d) Full sample.

Table 2 presents the values of the elastic and rheological parameters of the recycled polyvinyl chloride obtained using the proposed methodology at various temperatures.

Table 2. Elastic and rheological parameters of recycled polyvinyl chloride at different temperatures.

$T, ^\circ\text{C}$	20	30	40	50	60	70
E, MPa	1480	1450	1310	1210	1113	780
E_∞, MPa	5990	2970	1550	532	198	46.3
m^*, MPa	12.8	12.8	13.9	6.11	6.68	6.42
$\eta_0^*, \text{MPa} \cdot \text{minute}$	9.3×10^5	4.54×10^5	2.39×10^5	1.82×10^5	1.08×10^5	3.94×10^4

Figures 6–11 show the theoretical stress relaxation curves plotted according to the data in Table 2. The experimental points are marked with round markers. For all temperatures except for 70 °C, there was a good agreement between the theoretical curves and the experimental data. At high temperatures, there was a strong decrease in the elastic and rheological characteristics of the polyvinyl chloride, which explained the not entirely good agreement of the results at 70 °C.

**Figure 6.** Stress relaxation curve at $T = 20\text{ }^\circ\text{C}$.**Figure 7.** Stress relaxation curve at $T = 30\text{ }^\circ\text{C}$.

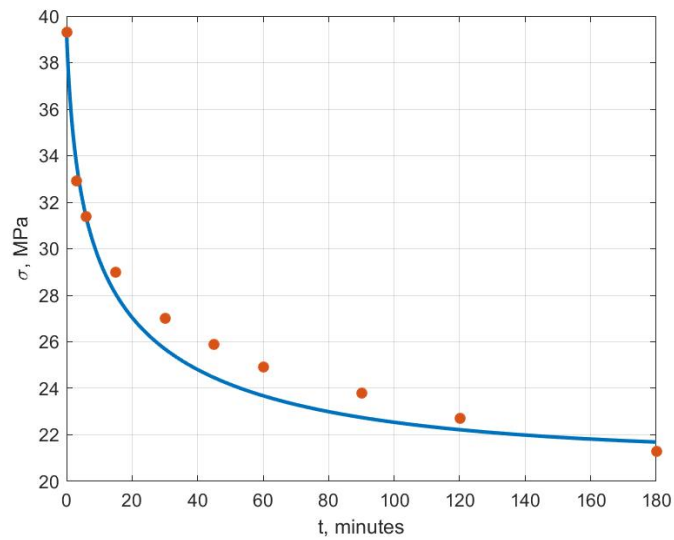


Figure 8. Stress relaxation curve at $T = 40\text{ }^{\circ}\text{C}$.

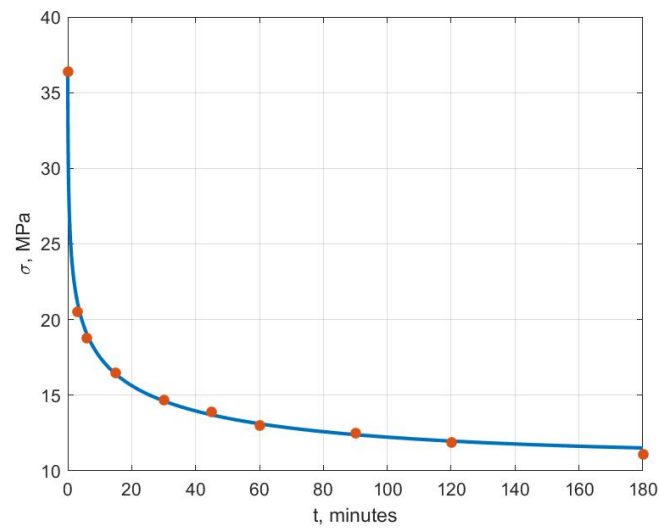


Figure 9. Stress relaxation curve at $T = 50\text{ }^{\circ}\text{C}$.

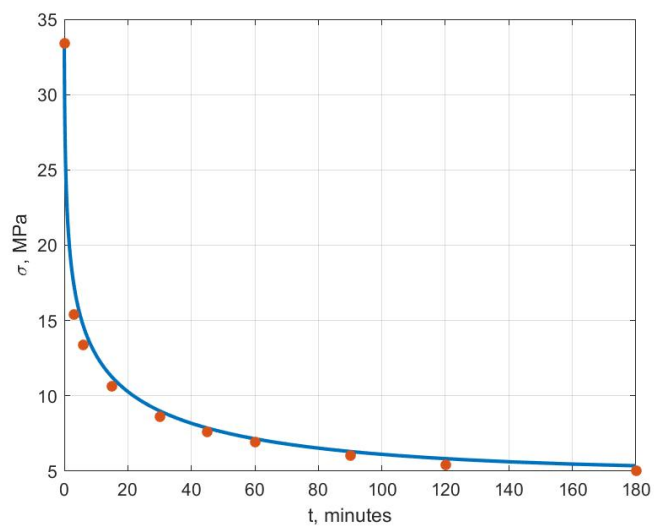


Figure 10. Stress relaxation curve at $T = 60\text{ }^{\circ}\text{C}$.

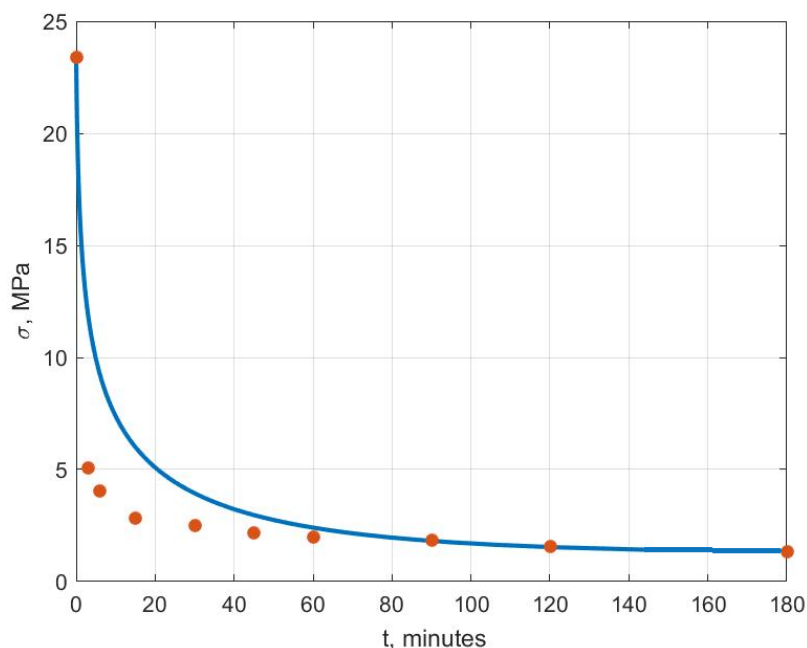


Figure 11. Stress relaxation curve at $T = 70\text{ }^{\circ}\text{C}$.

4. Discussion

In papers [16,17], the relaxation curves of the recycled polyvinyl chloride considered in this paper were processed earlier using a standard algorithm; in [30], nonlinear optimization methods were used to solve the same problem.

The values of the modulus of elasticity and the modulus of high elasticity obtained by us coincided with those given in [17] as machine learning methods were not used to determine them. A comparison of the values of the velocity modulus and the initial relaxation viscosity—obtained by the standard method using the methods of nonlinear optimization as well as using artificial neural networks—is shown in Figures 12 and 13. For temperatures of 20, 30 and 40 °C, the values of the velocity modulus and initial relaxation viscosity obtained using a neural network were close to the results based on the classical algorithm. At temperatures of 50 and 60 °C, the solution based on the neural network was closer to the solution using nonlinear optimization methods. At 70 °C, the value of the velocity modulus obtained based on the artificial neural network was approximately in the middle between the results based on the other two methods and the relaxation viscosity was closer to the solution using nonlinear optimization methods.

Table 3 presents a comparison of the coefficients of determination R^2 showing the quality of the approximation using three methods for six considered curves.

Table 3. Comparison of R^2 determination coefficients using three methods for determining the rheological parameters.

$T, \text{ }^{\circ}\text{C}$	20	30	40	50	60	70
R^2 Neural network	0.9772	0.9668	0.9693	0.9985	0.9899	0.7604
Classical algorithm	0.9798	0.9712	0.9811	0.9421	0.9450	0.7796
Nonlinear optimization	0.9918	0.9905	0.9909	0.9992	0.9994	0.9988

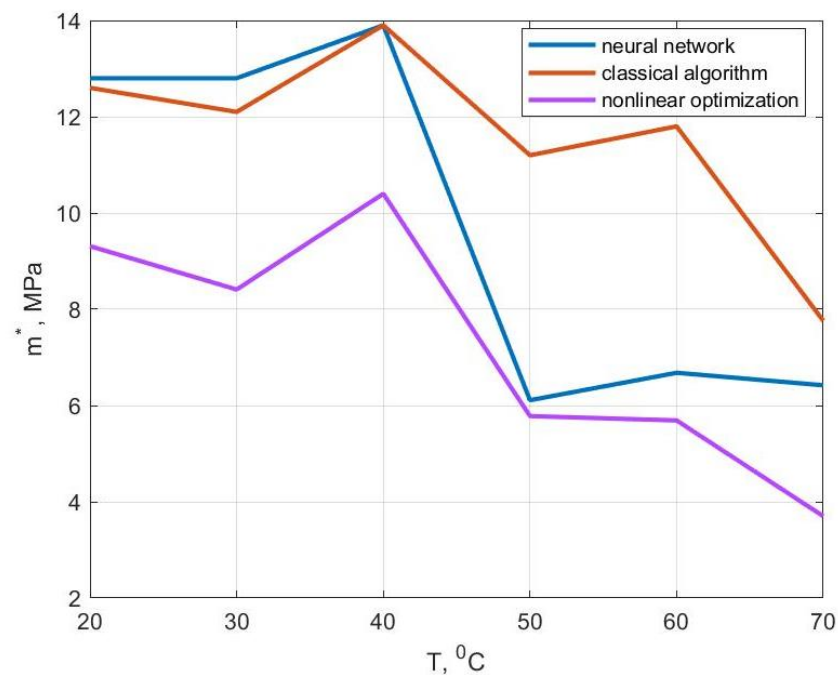


Figure 12. Comparison of the velocity modulus values obtained by different methods.

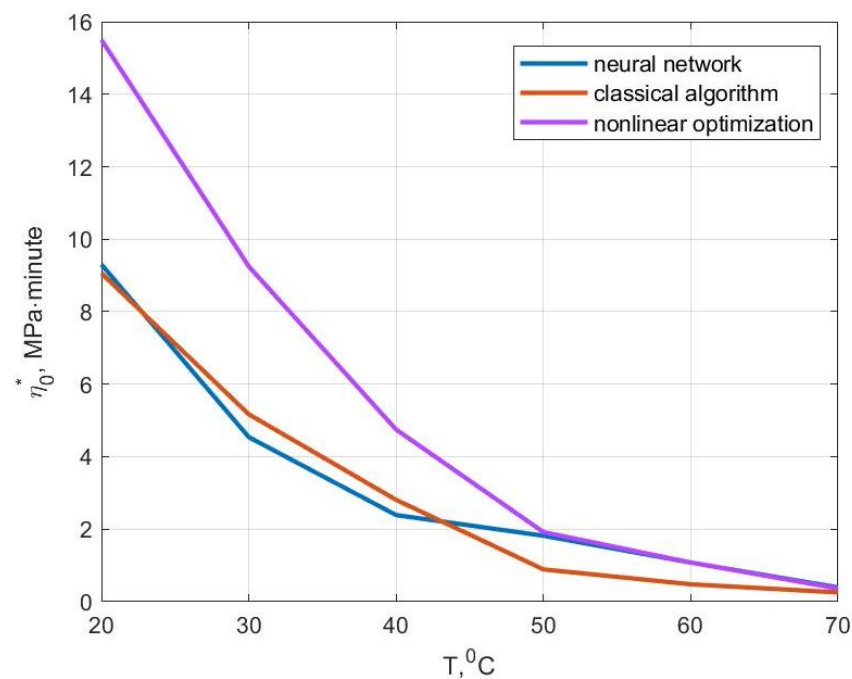


Figure 13. Comparison of the initial relaxation viscosity values obtained by different methods.

Table 3 shows that the efficiency of the neural networks and the classical algorithm was approximately the same. However, the classical algorithm used the numerical differentiation of the function $\sigma(t)$, which required a large number of points and the smoothing of the experimental curve. When using artificial neural networks, four characteristic points were sufficient and the smoothing of the experimental curve was not required. Nonlinear optimization methods are characterized by a higher quality of approximation; however, when using them, it is necessary to specify the initial approximation. If the real values of m^* and η_0^* are far from the initial approximation, then the solution may not be found.

Nonlinear optimization methods can be used to refine a solution obtained by the classical algorithm or with the help of artificial neural networks.

Note that the proposed technique based on machine learning methods, with a small adjustment, could be used not only for processing the stress relaxation curves of polymers, but also for processing creep curves. It is also possible to obtain the rheological parameters of materials from tests not only for tension, but also for other simple types of deformations such as shear, bending and torsion.

5. Conclusions

The possibility of applying machine learning methods to solve the problem of determining the rheological parameters of polymers from stress relaxation curves has been shown. An artificial neural network model was built to determine the rheological parameters of recycled PVC at various temperatures. The optimal number of neurons in the hidden layer of the network was determined. The approbation of the model showed a good quality of approximation of the experimental curves at temperatures from 20 to 60 °C. The efficiency of the artificial neural networks in determining the rheological parameters of the polymers was comparable with the efficiency of traditional algorithms. However, in comparison with traditional algorithms, the smoothing of the experimental curves was not required. The proposed technique made it possible to determine the rheological parameters of the polymers not only from stress relaxation experiments, but also from experiments on creep as well as experiments on types of deformation such as torsion, shear and bending.

Our further research will be aimed at testing the creep of polymer samples in bending and building neural networks to process these experiments. Further research could also be devoted to the choice of the optimal neural network architecture and the most effective algorithms for training.

Funding: This research received no external funding.

Institutional Review Board Statement: Not applicable.

Informed Consent Statement: Not applicable.

Data Availability Statement: Not applicable.

Acknowledgments: The author would like to acknowledge the administration of Don State Technical University for their resources and financial support.

Conflicts of Interest: The author declare no conflict of interest. The funders had no role in the design of the study; in the collection, analyses or interpretation of data; in the writing of the manuscript; or in the decision to publish the results.

References

1. Litvinov, S.V.; Yazyev, B.M.; Turko, M.S. Effecting of modified HDPE composition on the stress-strain state of constructions. *IOP Conf. Ser. Mater. Sci. Eng.* **2018**, *463*, 042063. [[CrossRef](#)]
2. Amjadi, M.; Fatemi, A. Creep and fatigue behaviors of High-Density Polyethylene (HDPE): Effects of temperature, mean stress, frequency, and processing technique. *Int. J. Fatigue* **2020**, *141*, 105871. [[CrossRef](#)]
3. Xiang, G.; Yin, D.; Meng, R.; Lu, S. Creep model for natural fiber polymer composites (NFPCs) based on variable order fractional derivatives: Simulation and parameter study. *J. Appl. Polym. Sci.* **2020**, *137*, 48796. [[CrossRef](#)]
4. Tezel, T.; Kovan, V.; Topal, E.S. Effects of the printing parameters on short-term creep behaviors of three-dimensional printed polymers. *J. Appl. Polym. Sci.* **2019**, *136*, 47564. [[CrossRef](#)]
5. Kuperman, A.M.; Turusov, R.A. Relaxation characteristics of reinforced plastics in tension of ring specimens by split disks. *Mech. Compos. Mater.* **2012**, *48*, 305–312. [[CrossRef](#)]
6. Askadskii, A.; Matseevich, T.; Gorbacheva, O.A. Stress relaxation of wood-polymer composites of savewood. *E3S Web Conf.* **2019**, *97*, 02044. [[CrossRef](#)]
7. Galitseiskii, K.B.; Timantsev, Y.A.; Dokuchaev, R.V.; Matseevich, T.A.; Buzin, M.I.; Piminova, K.S.; Askadskii, A.A. Compatibility of Components and Relaxation Properties of Composites Based on Secondary Polypropylene and Modified Basalt Fibers. *Polym. Sci. Ser. A* **2020**, *62*, 521–533. [[CrossRef](#)]
8. Matseevich, T.; Askadskii, A. Relaxation properties of organo-mineral composites. *IOP Conf. Ser. Mater. Sci. Eng.* **2018**, *365*, 042010. [[CrossRef](#)]

9. Afanasyev, E.S.; Goleneva, L.M.; Matseevich, T.A.; Askadskii, A.A. Synthesis and properties of a monolithic gradient polymer material based on polyurethane structures and 1, 4-butanediol as a chain extender. *Polym. Sci. Ser. A* **2017**, *59*, 12–26. [CrossRef]
10. Chepurnenko, V.; Yazyev, B.; Song, X. Creep calculation for a three-layer beam with a lightweight filler. *MATEC Web Conf.* **2017**, *129*, 05009. [CrossRef]
11. Trush, L.; Litvinov, S.; Zakieva, N.; Bayramukov, S. Optimization of the solution of a plane stress problem of a polymeric cylindrical object in thermoviscoelastic statement. In *Energy Management of Municipal Transportation Facilities and Transport*; Springer: Cham, Switzerland, 2017; pp. 885–893.
12. Tsybin, N.Y.; Turusov, R.A.; Andreev, V.I. Comparison of creep in free polymer rod and creep in polymer layer of the layered composite. *Procedia Eng.* **2016**, *153*, 51–58. [CrossRef]
13. Andreev, V.I.; Sereda, S.A. Calculation of an inhomogeneous polymer thick-walled cylindrical shell taking into account creep under the action of temperature load. *IOP Conf. Ser. Mater. Sci. Eng.* **2021**, *1015*, 012002. [CrossRef]
14. Litvinov, S.V.; Klimenko, E.S.; Kulinich, I.I.; Yazyeva, S.B. Longitudinal bending of polymer rods with account taken of creep strains and initial imperfections. *Int. Polym. Sci. Technol.* **2015**, *42*, 23–26. [CrossRef]
15. Litvinov, S.V.; Trush, L.I.; Yazyev, S.B. Flat axisymmetrical problem of thermal creepage for thick-walled cylinder made of recyclable PVC. *Procedia Eng.* **2016**, *150*, 1686–1693. [CrossRef]
16. Dudnik, A.E.; Chepurnenko, A.S.; Litvinov, S.V. Determining the rheological parameters of polyvinyl chloride, with change in temperature taken into account. *Int. Polym. Sci. Technol.* **2017**, *44*, 30–33. [CrossRef]
17. Chepurnenko, A.S.; Andreev, V.I.; Beskopylny, A.N.; Jazyev, B.M. Determination of Rheological Parameters of Polyvinylchloride at Different Temperatures. *MATEC Web Conf.* **2016**, *67*, 06059. [CrossRef]
18. Kubat, M. *Neural Networks: A Comprehensive Foundation*; Prentice Hall: Upper Saddle River, NJ, USA, 1999.
19. Elshamy, M.M.M.; Tiraturyan, A.N. Using application of an artificial neural network system to backcalculate pavement elastic modulus. *Russ. J. Build. Constr. Archit.* **2020**, *2*, 84–93. [CrossRef]
20. Elshamy, M.M.M.; Tiraturyan, A.N.; Uglova, E.V.; Zakari, M. Development of the non-destructive monitoring methods of the pavement conditions via artificial neural networks. *J. Phys. Conf. Ser.* **2020**, *1614*, 012099. [CrossRef]
21. Elshamy, M.M.M.; Tiraturyan, A.N.; Uglova, E.V. Evaluation of the elastic modulus of pavement layers using different types of neural networks models. *Adv. Eng. Res.* **2021**, *21*, 364–375. [CrossRef]
22. Sumpter, B.G.; Noid, D.W. Neural networks and graph theory as computational tools for predicting polymer properties. *Macromol. Theory Simul.* **1994**, *3*, 363–378. [CrossRef]
23. Duce, C.; Micheli, A.; Starita, A.; Tiné, M.R.; Solaro, R. Prediction of polymer properties from their structure by recursive neural networks. *Macromol. Rapid Commun.* **2006**, *27*, 711–715. [CrossRef]
24. Miccio, L.A.; Schwartz, G.A. From chemical structure to quantitative polymer properties prediction through convolutional neural networks. *Polymer* **2020**, *193*, 122341. [CrossRef]
25. Najjar, I.M.R.; Sadoun, A.M.; Abd Elaziz, M.; Abdallah, A.W.; Fathy, A.; Elsheikh, A.H. Predicting kerf quality characteristics in laser cutting of basalt fibers reinforced polymer composites using neural network and chimp optimization. *Alex. Eng. J.* **2022**, *61*, 11005–11018. [CrossRef]
26. Elsheikh, A.H.; Abd Elaziz, M.; Vendan, A. Modeling ultrasonic welding of polymers using an optimized artificial intelligence model using a gradient-based optimizer. *Weld. World* **2022**, *66*, 27–44. [CrossRef]
27. Elsheikh, A. Bistable Morphing Composites for Energy-Harvesting Applications. *Polymers* **2022**, *14*, 1893. [CrossRef]
28. Nikora, N.I.; Chepurnenko, A.S.; Litvinov, S.V. Determination of long-term critical loads for compressed polymer rods with nonlinear creep. *Eng. J. Don* **2015**, *34*, 19. Available online: <http://ivdon.ru/en/magazine/archive/n1p2y2015/2796> (accessed on 20 August 2022).
29. Solov'eva, E.V.; Askadskii, A.A.; Popova, M.N. Investigation of the relaxation properties of original and secondary polyvinylchloride. *Plast. Massy* **2013**, *2*, 54–62. Available online: <https://elibrary.ru/item.asp?id=18903261> (accessed on 20 August 2022).
30. Litvinov, S.V.; Yazyev, S.B.; Chepurnenko, A.S.; Yazyev, B.M. Determination of Rheological Parameters of Polymer Materials Using Nonlinear Optimization Methods. *Lect. Notes Civ. Eng.* **2020**, *130*, 587–594.